Stochastic Resonance in Electrical Circuits—II: Nonconventional Stochastic Resonance

Dmitrii G. Luchinsky, Riccardo Mannella, Peter V. E. McClintock, and Nigel G. Stocks

***Abstract*—Stochastic resonance (SR), in which a periodic signal in a nonlinear system can be amplified by added noise, is discussed. The application of circuit modeling techniques to the conventional form of SR, which occurs in static bistable potentials, was considered in a companion paper. Here, the investigation of nonconventional forms of SR in part using similar electronic techniques is described. In the small-signal limit, the results are well described in terms of linear response theory. Some other phenomena of topical interest, closely related to SR, are also treated.**

***Index Terms*—Fluctuations, noise, nonlinear.**

I. Introduction

IN AN EARLIER companion paper [1], the stochastic resonance (SR) phenomenon was introduced and reviewed briefly. It was pointed out that linear response theory (LRT) shows that SR need not be restricted to the systems with static bistable potentials in which it was originally discovered. It is to be anticipated in any system whose susceptibility increases rapidly with noise intensity. In the case of thermal equilibrium systems (e.g., those subject to white noise, in the absence of external forces), this means that the possibility of SR can be assessed by examination of the spectral density of fluctuations (SDF) in the absence of the weak periodic force. Where the SDF contains peaks that rise rapidly with noise intensity, the fluctuation dissipation relations show immediately that SR is to be anticipated.

In the next section, we consider several examples of nonconventional SR, both in the small signal limit where LRT is applicable and also for stronger signals where different theoretical approaches are required. In Section III, we describe some phenomena, closely related to SR, that have also been investigated through analog electronic experiments, and in Section IV, we draw conclusions.

Manuscript received April 13, 1999; revised June 7, 1999. This work was supported in part by the Engineering and Physical Sciences Research Council (U.K.), the Royal Society of London, the European Community, the International Science Foundation, INTAS, and the Russian Foundation for Fundamental Research. This paper was recommended by Associate Editor B. Linares-Barranco.

D. G. Luchinsky is with Department of Physics, Lancaster University, Lancaster LA1 4YB, U.K., and also with the Russian Research Institute for Metrological Service, Ozernaya 46, 119361 Moscow, Russia.

R. Mannella is with the Department of Physics, Lancaster University, Lancaster LA1 4YB, U.K., and also with the Dipartimento di Fisica, Università di Pisa and INFM UdR Pisa, Piazza Torricelli 2, 56100 Pisa, Italy.

P. V. E. McClintock is with Department of Physics, Lancaster University, Lancaster LA1 4YB, U.K.

N. G. Stocks is with the Department of Engineering, University of Warwick, Coventry CV4 7AL, U.K.

Publisher Item Identifier S 1057-7130(99)08024-6.

II. Unusual forms of Stochastic Resonance

A. SR for Coexisting Periodic Attractors

The system considered by Dykman *et al.* [2], [3] was the underdamped single-well Duffing oscillator

$$\ddot{x} + 2\Gamma\dot{x} + \omega_0^2 x + \gamma x^3 = F\cos\omega_F t + f(t) \qquad (1)$$

where the oscillator is driven by a periodic force of amplitude F, frequency ω_F, and $f(t)$ is the zero-mean white Gaussian noise of intensity D, such that

$$\langle f(t)\rangle = 0, \quad \langle f(t)f(t')\rangle = 4\Gamma D\delta(t-t'). \qquad (2)$$

The oscillator is driven by a nearly resonant force $F\cos\omega_F t$ with the frequency ω_F close to the oscillator eigenfrequency ω_0, such that

$$\Gamma, |\delta\omega| \ll \omega_F; \quad \gamma\delta\omega > 0; \quad \delta\omega = \omega_F - \omega_0. \qquad (3)$$

It is of particular interest in view of its importance in nonlinear optics [4]–[7] and its relevance to experiments on a confined relativistic electron excited by cyclotron resonant radiation [8], [9]. Provided that $F^2 \ll \omega_0^4(\delta\omega^2 + \Gamma^2)/|\gamma|$ and that the noise is weak, the resultant comparatively small amplitude ($\ll (\omega_0^2/|\gamma|)^{1/2}$) oscillations of $x(t)$ can conveniently be discussed in terms of the dimensionless parameters [10]

$$\eta = \Gamma/|\delta\omega|; \quad \beta = \frac{3|\gamma|F^2}{32\omega_F^3(|\delta\omega|)^3}; \quad \alpha = 3|\gamma|D/8\omega_F^3\Gamma \qquad (4)$$

which characterize, respectively, the frequency detuning, the strength of the main periodic field, and the noise intensity. The bistability [11] in which we are interested corresponds to a coexistence of stable states with large or small amplitude limit cycles, and it arises for a restricted range of η and β. The effect of weak noise $f(t)$ is to cause small vibrations about the attractors, and to induce occasional transitions between them within the bistable regime. Since the system is far away from thermal equilibrium, the transition probabilities are not given by the classical Kramers [12] theory. The inter-attractor transitions give rise to a stationary distribution of the oscillator over the attractors. They also give rise to an SR effect which, as we shall see, occurs in the close vicinity of the kinetic phase transition (KPT) [10], [13], where the stationary populations of the two attractors are equal, $w_1 \approx w_2$. The phenomenon can be discussed in terms of the LRT in [1, eqs. (16), (18)]; but, since the system now under consideration is of the nonequilibrium type, the susceptibility cannot now be obtained through the fluctuation dissipation relations of [1, eqs. (19), (20)].

1057–7130/99$10.00 © 1999 IEEE

Authorized licensed use limited to: Lancaster University Library. Downloaded on February 28,2010 at 05:33:11 EST from IEEE Xplore. Restrictions apply.

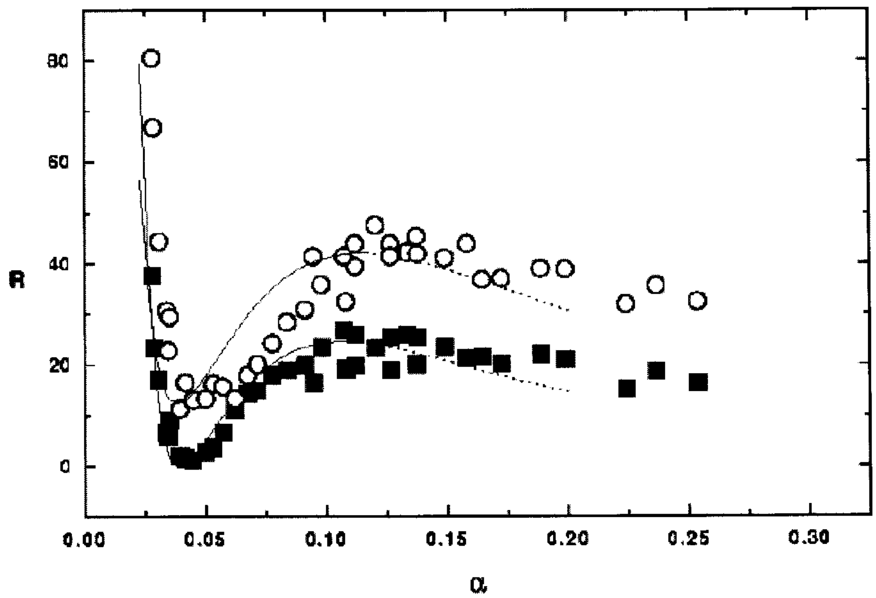

Fig. 1. The SNR R of the response of the system (1)–(3) to a weak trial force at frequency Ω, as a function of noise intensity α, in experiment and theory [2]: at the trial frequency Ω (circle data and associated theoretical curve); and at the "mirror-reflected" frequency $(2\omega_F - \Omega)$ (squares) . For noise intensities near those of the maxima in $R(\alpha)$, the asymptotic theory is only qualitative and so the curves are shown dotted.

Consider the response of the system (1) to an additional weak trial force $A\cos(\Omega t+\phi)$. Under stationary conditions, the response to this field in the presence of the strong driving force can still be described, in terms of linear response theory, by a susceptibility. The trial force beats with the main periodic force and thus gives rise to vibrations of the system, not only at Ω, but also at the combination frequencies $|\Omega \pm 2n\omega_F|$ (and also at $|\Omega \pm (2n+1)\omega_F|$ for a general nonlinearity). We are interested in the case where the strong and trial forces are both nearly resonant; that is, ω_F and Ω both lie close to the oscillator eigenfrequency ω_0. This is the case for which the response to the trial force is strongest. It is at its most pronounced at frequency Ω and at the nearest resonant combination, which for (1) is $|\Omega - 2\omega_F|$. The amplitudes of vibrations at these frequencies can be described respectively by susceptibilities $\chi(\Omega)$, $X(\Omega)$, so that trial-force-induced modification of the coordinate x, averaged over noise, can be sought in the form

$$\delta\langle x(t)\rangle = A\,\mathrm{Re}\{\chi(\Omega)\exp[-i\Omega t - i\phi] + X(\Omega)\exp[i(2\omega_F - \Omega)t] - i\phi]\}. \quad (5)$$

Within the KPT range, $|\mathrm{Im}\,\chi(\Omega)|$ displays a high narrow peak, whose width is given by the transition rates and is therefore strongly noise-dependent [10]. The rapid rise in susceptibility with noise intensity corresponds precisely to SR because, according to (5), the areas of the peaks in the power spectrum at frequencies Ω and $|\Omega - 2\omega_F|$ are

$$S(\Omega) = \frac{1}{4}A^2|\chi(\Omega)|^2, \quad S(|\Omega - 2\omega_F|) = \frac{1}{4}A^2|X(\Omega)|^2. \quad (6)$$

An intuitive understanding of the mechanism of stochastic amplification [14] can be gained by noting that the trial force modulates the driving force (and the coordinate $x(t)$) at frequency $|\Omega - \omega_F|$ and that, when $|\Omega - \omega_F|$ is small compared to the dynamical relaxation rate Γ, the dynamical response of the system is almost adiabatic. The beat envelope then results [2] in a slow oscillation in the amplitude of the force. This has the effect of strongly modulating the populations of the attractors (in the quasi-static limit). Such a modulation only occurs close to the KPT; away from the KPT line, the populations are always very different. If the noise intensity is optimally chosen, then the modulated system will have a tendency to make inter-attractor transitions *coherently*, once per half-cycle of the beat frequency. The net effect of the noise is, therefore, to increase the modulation depth of the beat envelope of the response, thereby increasing the components of the signal at frequencies Ω and $|\Omega - 2\omega_F|$.

The response of the system (1), (2), (4), and the variation of the signal-to-noise ratio (SNR) with α were investigated [2], [3] through analog experiments on the electronic model described in Section II-A of [1]. In terms of scaled units, the circuit parameters were set, typically, to $2\Gamma = 0.0397$; $\omega_0 = 1.00$; $\gamma = 0.1$; $\omega_F = 1.072\,00$; $\Omega = 1.070\,97$; and, to seek SR near the KPT, $F = 0.068$ and the amplitude of the trial force $A = 0.006$. The SNR's R, determined in the usual way from measurements of the delta spikes and the smooth background, are plotted (data points) as functions of noise intensity α in Fig. 1 for $\beta = 0.814$, $\eta = 0.236$. It is immediately evident that there is a range of α within which R *increases* with α. It is also apparent that, for both the main signal and that at the "mirror-reflected" combination frequency $2\omega_F - \Omega$, the form of $R(\alpha)$ in Fig. 1 is remarkably similar to that observed for conventional SR. A quantitative theory of the phenomenon is readily constructed through an extension [3] of the formalism introduced by Dykman and Krivoglaz [10]. It leads to the two full curves shown in the figure which, within experimental error, agree with the circuit data.

B. SR in Monostable Systems

In a noise-driven underdamped nonlinear oscillator [14], the natural frequency vibrations $\omega(E)$ depends on the energy

Authorized licensed use limited to: Lancaster University Library. Downloaded on February 28,2010 at 05:33:11 EST from IEEE Xplore. Restrictions apply.

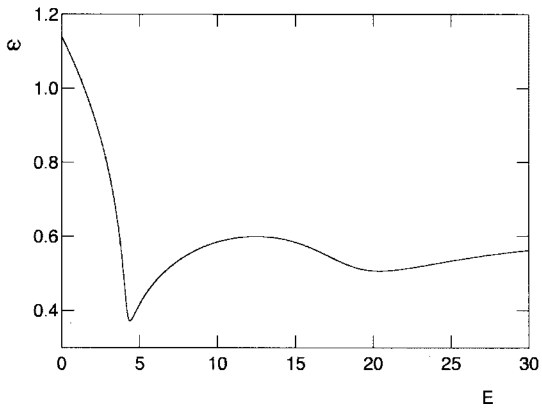

Fig. 2. Calculated variation of eigenfrequency $\omega(E)$ with energy E for the potential (7) with $B = 0.3, x_{\rm dc} = 0$ [23]. The first three extrema are at $\omega_{m1} = 0.372$, $\omega_{m2} = 0.600$, and $\omega_{m3} = 0.506$.

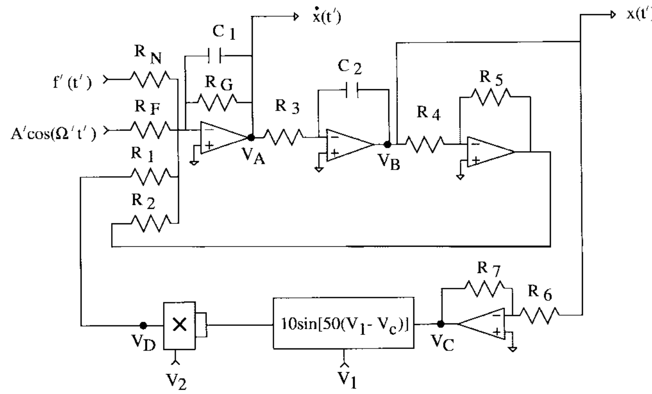

Fig. 3. Block diagram of the analog electronic circuit model of (7). Its behavior can conveniently be analyzed in terms of the voltages V_A, V_B, V_C, and V_D at the points indicated (see text) [23].

E (measured from the bottom of the potential well). The oscillator has a (Boltzmann) distribution over energy, and therefore over frequency. With increasing noise intensity this distribution changes and the response at certain frequencies can become strongly enhanced by noise. The appearance of an additional *zero-dispersion* spectral peak (ZDP), where the damping is extremely small and $\omega(E)$ is nonmonotonic as a function of energy, was predicted and discussed by Soskin [15], [16]. The exponential rise in the ZDP with increasing noise intensity can be expected, on the basis of (18)–(20) of [1], to give rise to SR at nearby frequencies.

The model used for the original prediction and first observation of SR in monostable systems [17], [18] was the tilted single-well Duffing oscillator driven by Gaussian white noise plus a weak periodic force. However, much stronger SR effects are to be anticipated in underdamped SQUID's, which we now consider, even for relatively large values of Γ. The dynamics of the magnetic flux through a periodically-driven SQUID loop can be described in terms of a resistively shunted model [19] whose governing equation, after appropriate changes of variable (e.g., see [20]) can be written

$$\begin{aligned}\ddot{x} + 2\Gamma\dot{x} + \frac{dU}{dx} &= f(t) + A\cos(\Omega t)\\ U(x) &= \frac{1}{2}B(x - x_{\rm dc})^2 - \cos x\\ \langle f(t)\rangle = 0, \quad \langle f(t)f(t')\rangle &= 4\Gamma D\delta(t - t')\end{aligned} \tag{7}$$

corresponding to classical motion in the potential $U(x)$ under influence of the additive noise $f(t)$. We consider the case where the amplitude A of the periodic force is small, where the constant Γ is also small so that motion in the potential is underdamped, and where the relative magnitudes of the constants B and $x_{\rm dc}$ are such that the potential has a single potential well.

The corresponding $\omega(E)$ dependence calculated for the SQUID potential (7) with $B = 0.3$ and $x_{\rm dc} = 0$, shown in Fig. 2, exhibits a local maximum and two local minima within the range plotted. Each of these extrema may be expected to produce a ZDP in $Q^{(0)}(\omega)$ that could in principle give rise to SR. This inference [20] was tested with an analog electronic model of (7), as shown in block form in Fig. 3. $A'\cos\Omega't'$ and $f'(t')$ are respectively a signal and an external noise applied to the underdamped nonlinear oscillator. A' is the amplitude of the signal in volts, $f'(t')$ is the value of the noise voltage applied to the circuit, and Ω' and t' are the real frequency and time in units of Hertz and seconds. Setting to zero the total currents at the inputs of the operational amplifiers whose outputs are V_A and V_B respectively, we obtain

$$\begin{aligned}&\frac{V_A}{R_G} + C_1\frac{dV_A}{dt'} + \frac{f'(t')}{R_N} + \frac{A'\cos(\Omega't')}{R_F} - \frac{(R_5/R_4)V_B}{R_2}\\ &\qquad + \frac{V_D}{R_1} = 0\end{aligned} \tag{8}$$

$$C_2\frac{dV_B}{dt'} + \frac{V_A}{R_3} = 0. \tag{9}$$

The trigonometric integrated circuit (IC) was configured to give an output of $10\sin[50(y_1 - y_2)]$, where the two inputs y_1 and y_2 are in volts and the argument of the sine is in degrees. The IC operation is restricted to lie within the range ±500°. In order to increase the dynamic range of x encompassed by the model, an analog multiplier was used as shown to convert the argument to the double angle. The voltage at its output, in terms of the voltage V_C at the input of the trigonometric IC and the constant voltages V_1 and V_2, and allowing for internal scaling by a factor of 0.1, is

$$V_D = 0.1[10\sin(50(V_1 - V_C))]^2 + V_2 \tag{10}$$

or, in terms of the double angle now expressed in radians

$$V_D = 5\Big(1 - \cos\Big[\frac{\pi}{1.8}(V_1 - V_C)\Big]\Big) + V_2. \tag{11}$$

The voltage V_C is just

$$V_C = -\frac{R_7}{R_6}V_B. \tag{12}$$

Eliminating V_A, V_C, and V_D from (8), (9), (11), and (12), and writing $V_B \equiv x$, the differential equation for the voltage x in the circuit can therefore be written

$$\begin{aligned}&R_1C_1R_3C_2\frac{d^2x}{dt'^2} + \frac{R_1}{R_G}R_3C_2\frac{dx}{dt'} + \frac{R_1R_5}{R_2R_4}x\\ &\quad - 5\Big(1 - \cos\Big[\frac{\pi}{1.8}\Big(V_1 + \frac{R_7}{R_6}x\Big)\Big]\Big) - V_2\\ &\quad = \frac{R_1}{R_F}A'\cos\Omega't' + \frac{R_1}{R_N}f'(t')\end{aligned} \tag{13}$$

Authorized licensed use limited to: Lancaster University Library. Downloaded on February 28,2010 at 05:33:11 EST from IEEE Xplore. Restrictions apply.

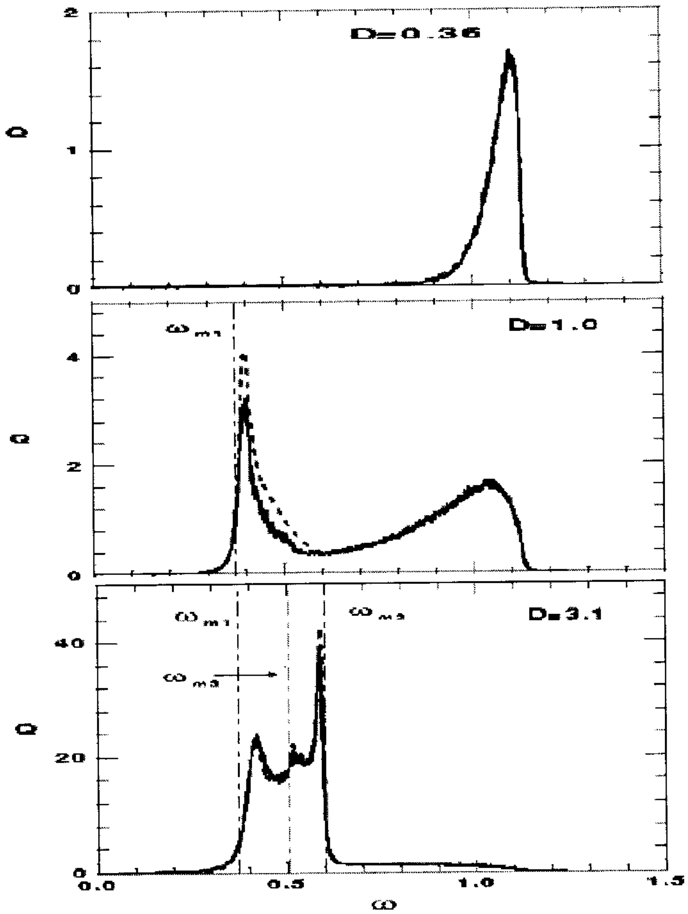

Fig. 4. Spectral density of fluctuations $Q(\omega)$ measured (jagged lines) for the analog electronic model of (7) with $A = 0$, $B = 0.3$, $x_{\rm dc} = 0$, compared with the calculated behavior (dashed curves), for three noise intensities D[23]. One ZDP is seen for $D = 1.0$, and three for $D = 3.1$. Note the differing ordinate scales.

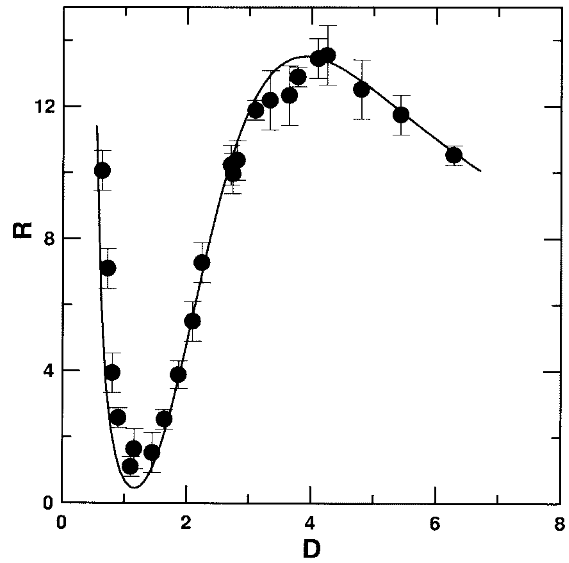

Fig. 5. Signal/noise ratio R measured (data points) as a function of noise intensity D for the analog electronic model of (7) with $A = 0.016$, $\Omega = 0.62$, $B = 0.3$, $x_{\rm dc} = 0$, compared with the behavior predicted (full curve) by LRT, [1, eqs. (18)–(20)], using the calculated spectraldensities $Q(\omega)$, of which three examples are plotted as dashed lines in Fig. 4 [23].

where we have chosen: $R_N = R_F = 100$ kΩ; $R_1 = R_3 = 100$ kΩ; $R_4 = R_5 = R_6 = 10$ kΩ; $R_7 = 11.459$ kΩ; $R_G = 22$ MΩ; $C_1 = C_2 = 10$ nF; $V_1 = -0.9$ V. The multiwell and single-well cases of the potential (7) correspond to different values of the parameters R_2 and V_2. For example, on introducing $R_2 = 100\,\text{k}\Omega$, $V_2 = -3.93$ V, the time constant $\tau' = R_1C_1/\sqrt{5} = R_3C_2/\sqrt{5}$ and the damping constant $\Gamma' = R_1/(R_G\sqrt{5})$, (13) can be reduced to

$$\tau'^2\ddot{x} + \Gamma'\tau'\dot{x} + 0.2(x - 1.07) + \sin(2x) = 0.2A'\cos\Omega't' + 0.2f'(t') \quad (14)$$

whose parameters are readily related to those in the model (7) by means of the scaling relations

$$x \to 2x, \quad \tau = \frac{\tau'}{\sqrt{2}}, \quad t = \frac{t'}{\tau}, \quad \Omega = \Omega'\tau, \quad \Gamma = \Gamma'\sqrt{2}$$

with $B = 0.1$, $x_e = 2.14$, $A = 0.2A'$, $f(t) = 0.2\sqrt{2}f'(t')$. The nominal value of 2Γ was 0.001 44; the actual value, measured experimentally by two independent methods [21], was found to be $2\Gamma = 0.0011$.

When the model was driven by quasi-white noise from an external noise generator, with $A = 0$, the measured spectral density $Q^{(0)}(\omega)$ underwent dramatic changes of shape with increasing D, as shown in Fig. 4. The three ZDP's appeared sequentially as D "tuned" the oscillator to different ranges of $\omega(E)$. When the weak periodic force $A\cos(\Omega t)$ was also added, with Ω chosen to lie close to the frequency of the local maximum of $\omega(E)$ and the corresponding ZDP where $|\chi|$ is expected to be strongly noise dependent, the SNR was found to vary with increasing D, as shown by the data points of Fig. 5. At first the SNR falls, as one might expect on intuitive grounds; but there follows a range of D within which the SNR markedly *increases* with increasing D, i.e., a strong manifestation of SR, before falling again at very high D. The theory of these phenomena, developed [20], [22], [23] on the usual LRT basis and shown by the full curves of Figs. 4 and 5, is in satisfactory agreement with the measurements. Note that if Γ is made small enough, there is in principle no limit to the rise in SNR that can be achieved, and that zero-dispersion SR also occurs in SQUID's with multiwell potentials [22], [23] where it exhibits some interesting features.

These circuit measurements strongly imply that zero-dispersion SR is to be anticipated in underdamped SQUID's. The performance of a high-frequency SR device based on an underdamped SQUID would probably be comparable with that of low-frequency SQUID-SR devices [24], and it would have the additional advantage of being tunable over a wide range of frequencies by adjustment of the static magnetic field and/or the inductance of the loop.

C. SR for Periodically Modulated Noise Intensity

SR phenomena can also arise [25] in a bistable system when the noise and the periodic force are introduced multiplicatively, so that the former is modulated by the latter. Periodically modulated noise is not uncommon and arises, for example, at the output of any amplifier (e.g., in optics or radio-astronomy) whose amplification factor varies periodically with time. It is of obvious importance, therefore, to establish whether or

Authorized licensed use limited to: Lancaster University Library. Downloaded on February 28,2010 at 05:33:11 EST from IEEE Xplore. Restrictions apply.

not a modulated zero-mean noise can give rise to a periodic signal in the system it is driving. Such an effect would not, of course, occur in a linear system where the signal is directly proportional to the driving noise so that they must both, on average, vanish. In a *nonlinear* system, however, a periodic signal does arise; furthermore, where the system is bistable a form of SR can occur for periodically modulated noise intensity. It has some novel features that are strikingly different from those in conventional SR. Dykman *et al.* [25] addressed the problem through analytic approximation and an electronic model of an overdamped Brownian particle in moving in an asymmetric bistable potential

$$\begin{aligned}\dot{x} + U'(x) &= f(t)\\ &\equiv \left(\frac{1}{2}A\cos(\Omega t) + 1\right)\xi(t)\\ U(x) &= -\frac{1}{2}x^2 + \frac{1}{4}x^4 + \lambda x. \end{aligned} \tag{15}$$

Here, λ characterizes the asymmetry of the potential. For $-2/(3\sqrt{3}) < \lambda < 2/(3\sqrt{3})$ the potential $U(x)$ has two minima, i.e., the system is bistable. The function $\xi(t)$ represents white Gaussian noise of intensity D, so that

$$\langle f(t)f(t')\rangle = 2D\delta(t-t')\left[1 + A\cos(\Omega t) + \frac{A^2}{8}(1+\cos(2\Omega t))\right] \tag{16}$$

i.e., the intensity of the driving force $f(t)$ is periodic in time. The modulation was assumed to be weak, $A \ll 1$, so that the term in A^2 in (16) could be neglected.

Both the approximate theory and measurements of signal/noise ratio R in the electronic model immediately demonstrated [25] the occurrence of SR: the rate of increase of R was faster than D, so that it did not represent merely the proportionality of the modulation to D in (16). The most striking feature was that the SR effect occured *only* when the bistable potential was made asymmetric, with wells of different depths, whereas conventional SR can be regarded (see above) as a kinetic phase transition (KPT) phenomenon that is at its most pronounced for equally populated stable states i.e., for equal well depths.

D. SR in Threshold Devices

It is interesting to notice that the first experimental evidence of SR was obtained in an electronic bistable system working as a threshold detector (a Schmitt trigger) [26]. The electronic device used was fairly simple, consisting of an operational amplifier with feedback, subject to random noise and a periodic forcing. Although the work of [26] was prompted by [27], so that the authors had in mind a continuous system, they realized that their system had hysteresis and was actually behaving more like a threshold system.

After a period during which work on SR was focused mainly on continuous systems, SR in threshold systems again became of interest when it was realized that the latter were perhaps more appropriate for the description of neuronal dynamics. At the same time, in an attempt to work on minimal systems able to display SR, attention turned to the so-called level crossing detector (LCD), which is basically a threshold device. The new wave of electronic simulations and theoretical explanations for this class of system were reviewed in [28], [29]. A fairly general theoretical approach able to account for their behavior in terms of simple quantities was developed in [30]. It was soon realized, however, that the dynamics of this class of systems is closely connected to the dithering effect, already well known in digital signal processing, as explained in [31].

More recently, SR in threshold devices has been rediscovered in an electronic simulation [32]; the authors study a two-state threshold comparator fed by white noise and a periodic signal; they show that the cross-correlation between output and input can be enhanced in the appropriate range of input noise intensity.

E. Aperiodic SR and Information Transmission

Traditionally, SR has been quantified in terms of a noise-induced maximum in the SNR [1]. For systems subject to a periodic signal, this is a simple and convenient quantity to measure experimentally. The output signal power and background noise intensity can easily be determined from a measurement of the power spectrum of the response. However, spectral methods cannot be easily applied if the input signal is broadband. Recently, SR has been extended to encompass broadband signals [33], so-called *aperiodic SR*. Although the term was first coined in a study of a parallel array, it was already known that broadband signals could exhibit SR type effects [34], [35]. In fact, aperiodic SR can occur in any system that displays conventional SR.

Due to the broadband nature of the signals, information-theoretic measures have started to be employed. The most commonly used measure is the average mutual information [35]–[40], although other quantities have also been considered [41].

Using this type of approach, the SR system is treated as a noisy communication channel with an input signal $x(t)$ and an output $y(t)$. The average mutual information (transmitted information) $I(x;y)$ is then computed for these quantities. For threshold-type systems, such as a simple comparator or Schmitt trigger, there often exists a countable number of output states. In this case the system can be treated as a semi-infinite channel. The average mutual information is then given by

$$\begin{aligned} I &= H(y) - H(y \mid x)\\ &= -\sum_{n=0}^{N} P_y(n)\log_2 P_y(n)\\ &\quad - \left(-\int_{-\infty}^{\infty} P_x(x)\,dx \sum_{n=0}^{N} P(n \mid x)\log_2 P(n \mid x)\right). \end{aligned} \tag{17}$$

$H(y)$ is the information content (or entropy) of $y(t)$ and $H(y \mid x)$ can be interpreted as the amount of encoded information lost in the transmission of the signal. Enumerating the possible output states by n, where $n = 0, 1, \cdots, N$ (N being the number of output levels), $P_y(n)$ is then the probability of the

Authorized licensed use limited to: Lancaster University Library. Downloaded on February 28,2010 at 05:33:11 EST from IEEE Xplore. Restrictions apply.

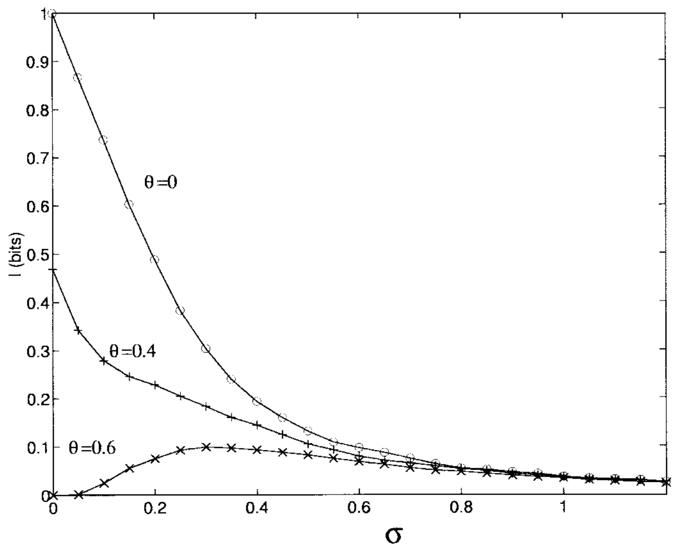

Fig. 6. Plot of the transmitted information against σ for three different settings of the threshold, $\theta = 0$ (circles), $\theta = 0.4$ (pluses), and $\theta = 0.6$ (crosses). The data points are from digital simulations and the solid lines are guides to the eye.

output $y(t)$ being in state n and $P(n \mid x)$ is the conditional probability density given knowledge x.

To illustrate the use of this approach, consider what happens in a simple comparator circuit. It is assumed that two possible output states exist, labeled 0 and 1. In the absence of any noise, state 1 is accessed if the signal $x(t)$ exceeds the threshold level θ; otherwise, the system remains in state 0. If noise $\eta(t)$ is now added to the signal, the system will only change state when both the signal plus the noise exceeds θ.

Fig. 6 shows results from a digital simulation of this model. The signal was uniformly distributed between the limits ± 0.5 and the noise was Gaussianly distributed with standard deviation σ. It can be seen that SR effects (a maximum in the transmitted information) are observed when the signal is entirely subthreshold i.e., when $\theta > 0.5$.

The appearance of SR can be understood as follows. If all information is lost in transmission, $H(y \mid x) = H(y)$ (which occurs as $\sigma \to \infty$), and hence $I = 0$. Alternatively, if all encoded information is transmitted, $(\sigma = 0)$, $H(y \mid x) = 0$, and $I = H(y)$. Given that it is straightforward to show that for any non-zero σ, $H(y \mid x) < H(y)$, it would seem to follow that maximum information transfer occurs when there is no internal noise. However, as we have seen, this is not necessarily the case. This is because internal noise also serves to increase $H(y)$. In effect, when the signal is subthreshold, the noise facilitates access to additional bits of information. Consequently, the maximization of I by internal noise is a balance between additional information generated by the noise and the increased loss in information transmitted through the system with increasing σ.

It should be noted that this is not the only way of defining I. In neurophysiological experiments, it is common practice to measure the time between successive firings of a neuron. The same idea can be applied to simple threshold systems by measuring the time between generated events; this gives rise to a set of times $\{\tau_i\}$. This enables the average mutual information $I(x; \{\tau_i\})$ to be constructed. A number of authors have used this approach to make connection with neurophysiological applications [35]–[37]. Similar SR type effects are observed using this approach.

F. SR in Networks

To date, the majority of studies on SR have tended to focus on the dynamics of single elemental systems. However, recently there has been a growth of interest in connecting together a number of such elemental systems to form arrays or networks. A wide range of network design, using different elements and connectivity, has been investigated; these include, globally coupled networks [42]–[45], randomly connected networks [46], linear chains [47]–[53] and parallel arrays [33], [54]–[58]. Possible applications include pattern segmentation [59], perceptual interpretation of ambiguous figures [60], the modeling of biological sensory system [33], [55], modeling of neuropsychiatric disorders [61], and nanoscale subthreshold magnetic field detection [62].

Studies of networks have demonstrated that SR is not solely a temporal effect, it can also manifest itself in the spatiotemporal domain. Indeed, the global response of a network can lead to an enhanced SR effect, as exemplified in array-enhanced SR (AESR) [47]. The existence of AESR, which occurs in a linear chain of coupled bistable oscillators, has recently been confirmed experimentally in a diode resonator connected diffusively into an array of nonidentical resonators [48], [50], [51]. In these systems, in addition to the usual temporal synchronization, a spatial synchronization of the chain to the signal also occurs. The maximum in the SNR is observed to coincide with the optimal spatiotemporal synchronization of the chain [48]. Similar enhancements of the SR effect have also been found in globally coupled networks [42], [43]. Again, SR enhancements over and above that displayed by a single element were observed.

The motivation behind studying parallel arrays of elements comes primarily from neurophysiological applications. Sensory neurons tend to be arranged in a highly parallel structure. They also possess significant amounts of internal noise and are highly nonlinear. Consequently, they have all the features necessary for exhibiting SR. Indeed, SR type effects have been observed in a number of real neurophysiological experiments [63], [64].

Parallel arrays differ from other types of network in that the elements are not actually coupled. Generally, each element is subject to the same signal but evolves under the influence of its own internal noise. The elements are only connected at a common summing point. The action of the summing point leads to an ensemble averaging over the noise. Consequently, the SNR at the output can be simply improved by increasing the number of elements. In addition to displaying SR, the dynamics of each element linearises with increasing noise intensity (see Section III-B). Therefore, such arrays are capable of transmitting a high-fidelity reproduction of the signal, despite the nonlinearity of individual elements. It is the ability of these arrays, to display SR effects *and* a high-fidelity linear response, that makes them so intriguing as signal processing systems.

Authorized licensed use limited to: Lancaster University Library. Downloaded on February 28,2010 at 05:33:11 EST from IEEE Xplore. Restrictions apply.

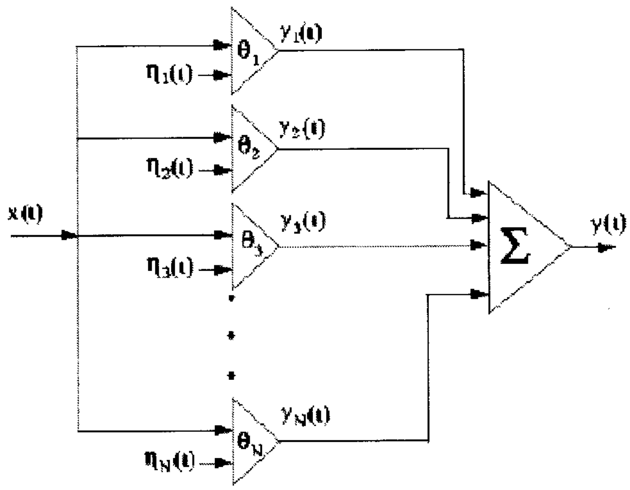

Fig. 7. A summing network of N threshold devices. Each device is subject to the same signal (a Gaussianly distributed signal with zero mean and standard deviation σ_x) but independent Gaussian noise.

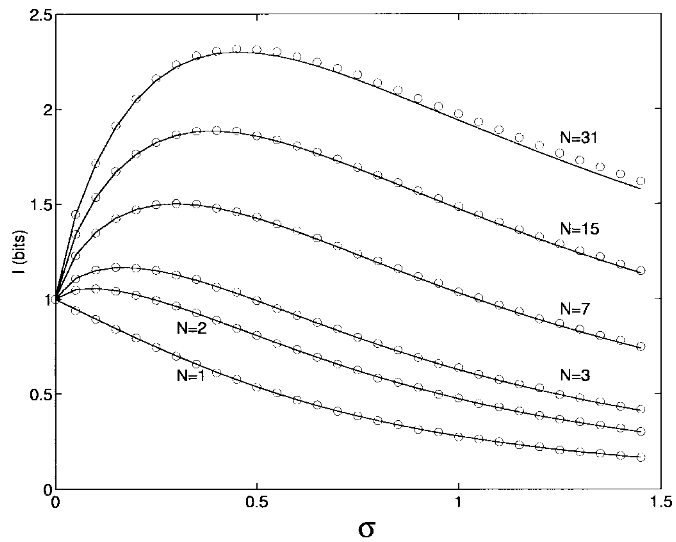

Fig. 8. Plot of transmitted information against $\sigma = \sigma_\eta/\sigma_x$ for various N and all $\theta_i = 0$. The data points are the results of a digital simulations of the network and the solid lines were obtained by numerically evaluating (19).

G. Suprathreshold SR

SR is commonly understood to be the enhancement, by noise, of the response of a system to a *weak* signal [1]. By weak, one normally means with reference to an appropriate scale of the system. In a threshold-type system, the scale would be taken as the threshold level. Normally, SR is only observed if the signal is smaller than this scale i.e., it is subthreshold. For signals of sufficient magnitude, the SR effect disappears. However, it has recently been observed [65] that, in parallel networks of threshold devices, SR-type effects can occur for any magnitude of signal—including suprathreshold signals. For this reason, this form of SR has been termed suprathreshold SR (supra-SR).

Consider the summing network of N threshold devices shown in Fig. 7. Each threshold device is subject to the same input signal $x(t)$ but to an independent Gaussian noise $\eta_i(t)$, with a standard deviation σ_η. The devices are modeled as Heaviside functions, the outputs $y_i(t)$ being given by the response function

$$y_i(t) = \begin{cases} 1, & \text{if } x(t) + \eta_i(t) > \theta_i \\ 0, & \text{otherwise} \end{cases} \tag{18}$$

where θ_i are the threshold levels and $i = 1, 2, \cdots N$. The response of the network is obtained by summing the individual responses of each device. Consequently, $y(t)$ is the number of devices that are triggered at any instant of time.

Although other studies have considered similar networks [33], this model differs in that each threshold can be chosen independently. This enables the thresholds to be adjusted to optimize the information transmission for a given signal distribution. Uniformly placing the thresholds across the signal space mimics the signal encoding abilities of a flash analog-to-digital converter (ADC)—this is the optimal threshold distribution for a uniformly distributed signal. For other signal distributions, the optimal threshold distribution can be found using the method of *optimal quantization* [65]–[67]. If such a procedure is undertaken, one finds that the transmitted information is generally maximized at zero levels of noise.

However, this is not the case if every threshold is adjusted to coincide with the dc component of the signal. Fig. 8 illustrates what happens for a broadband Gaussianly distributed input signal with standard deviation σ_x and zero mean. Each threshold level θ_i has been set to zero to coincide with the mean of the signal. It can be seen that an SR-type effect is observed, providing $N > 1$, even though the signal is suprathreshold. Indeed, it was found that the effect remained for any magnitude of signal. Consequently, in contrast to single element threshold systems, noise can optimize the performance of parallel arrays to suprathreshold as well as to subthreshold signals.

The mechanism giving rise to supra-SR is quite different to that of conventional SR. In the absence of noise, all devices switch in unison and consequently the network acts like a single-bit ADC ($I = 1$). Finite noise results in a distribution of thresholds that gives access to more bits of information; effectively the noise is accessing more degrees of freedom of the system, and hence, generating information. Using (17), $I(x; y)$ can be calculated analytically to give

$$\begin{aligned} I = &-\sum_{n=0}^{N} P_y(n) \log_2 P'(n) \\ &- \left(-N \int_{-\infty}^{\infty} dx\, P_x(x)(P_{1|x} \log_2 P_{1|x} \right. \\ &\left. + P_{0|x} \log_2 P_{0|x})\right) \\ P'(n) = &\int_{-\infty}^{\infty} dx\, P_x(x) P_{1|x}^n P_{0|x}^{N-n} \end{aligned} \tag{19}$$

where $P_y(n) = C_n^N P'(n)$, C_n^N is the Binomial coefficient. The signal distribution, $P_x(x) = (1/\sqrt{2\pi\sigma_x^2}) \exp(-x^2/2\sigma_x)$, and $P_{1|x} = 1/2\, \mathrm{Erfc}[(\theta - x)/\sqrt{2\sigma_\eta^2}]$ is the conditional probability of $y_i = 1$ for a given x (note all devices are identical) and similarly $P_{0|x} = 1 - P_{1|x}$ is the probability of a zero given x. Erfc is the complementary error function [68]. The integrals and summation were calculated numerically to give the solid

Authorized licensed use limited to: Lancaster University Library. Downloaded on February 28,2010 at 05:33:11 EST from IEEE Xplore. Restrictions apply.

lines in Fig. 8. Good agreement between simulation and theory is obtained confirming the suprathreshold SR effect.

Such networks could have direct engineering applications. This is particularly true in the design of ADC's when the signal is highly nonstationary and weak with respect to the internal noise of the system. The nonstationarity of the signal precludes the possibility of fixing the threshold levels in an optimal configuration. In this situation, some advantage can be gained by simply adjusting the levels to coincide with the mean of the signal and exploiting the supra-SR effect [69].

III. Related Phenomena

A. Noise-Enhanced Heterodyning (NEH)

In the well-known phenomenon of heterodyning, two high-frequency fields—an "input signal" and a "reference signal"—are mixed nonlinearly to generate a heterodyne signal at the difference frequency. The addition of noise usually results in a decrease in the amplitude of the heterodyne signal (and its SNR), because the frequency response of the system becomes correspondingly broadened. Nonetheless, it has been shown [70] that, in bistable systems of the kind that exhibit SR, the heterodyne signal (and SNR) can sometimes be enhanced by an increase in the noise intensity. Consider an overdamped bistable system driven by three time-dependent forces representing respectively the reference and input signals, and noise

$$\frac{dx}{dt} = -U'(x) + A_{\rm ref} x \cos\omega_0 t + A_{\rm in}(t)\cos(\omega_0 t + \phi(t)) + f(t). \tag{20}$$

Here, the terms $\propto A_{\rm ref}$ and $\propto A_{\rm in}(t)$ are respectively the high-frequency reference signal corresponding to a local oscillator of frequency ω_0 (applied multiplicatively), and the modulated high-frequency input signal (applied additively). The functions $A_{\rm in}(t)$ and $\phi(t)$ vary slowly compared to $\cos\omega_0 t$, and it is their variation in time that has to be revealed via heterodyning. The heterodyning can be characterized by the low-frequency signal at the output, $x^{(\rm sl)}(t) = \overline{x(t)}$ (the overbar stands for averaging over the period $2\pi/\omega_0$), for $A_{\rm in} = \rm const$ and $\phi = \Omega t + \rm const$, with $\Omega \ll \omega_0$, i.e., for a monochromatic input signal whose frequency $\omega_0 + \Omega$ is slightly different from the frequency ω_0.

Dykman *et al.* [70] considered the case where the double-well potential $U(x)$ has equally deep wells, as in standard SR, and for convenience chose it to be the quartic potential

$$U(x) = -\frac{1}{2}x^2 + \frac{1}{4}x^4. \tag{21}$$

For the case where $A_{\rm in}(t)$, $\phi(t)$ vary slowly over the time t_r, the equations describing the dynamics of the system turn out to be identical to those of conventional SR. The system can thus be well-described in terms of LRT provided only that A is small enough. It was thus demonstrated theoretically and by use of a circuit model that, in close analogy to conventional SR, NEH in a bistable system can produce a very substantial enhancement of the heterodyne signal over that obtained by heterodyning in e.g. a single-well nonlinear system.

Building on the understanding gained from studies of the analog electronic model, both SR and NEH were subsequently observed in a nonlinear optical system [71], [72].

B. Noise-Induced Linearization

The phenomenon of *noise-induced linearization* was identified in the course of experiments on SR, using analog electronic models [73]. The unexpected observation was that the signal distortion introduced by passage through a nonlinear system could be reduced by the addition at the input of external white (or weakly colored) noise of sufficient intensity. The scenario was found to hold experimentally for many different nonlinear systems, including monostable as well as bistable, underdamped as well as overdamped, chaotic as well as regular, and for signals of various shapes. Because the resultant linearized output $x(t)$ is inevitably noisy, we consider how the ensemble average $\langle x(t)\rangle$ of the output varies with relevant parameters, for example with the noise intensity at the input.

The basic idea of linearization by added noise is, of course, already familiar from specific observations and applications in science and engineering, e.g. the removal of digitization steps in the output of an ADC, or the linearization of periodic signals in neurophysiological experiments [74], or the linearization of the response of ring-laser gyroscopes at low angular velocities [75]. The results under discussion suggested, however, that noise-induced linearization may exist as a more general phenomenon than had been appreciated, thus further illustrating the idea [76] that the role of noise in a dynamical system may often be, in a sense, creative.

The linearization occurred in two different senses. First, a sinusoidal input was able to pass through the system without significant change of shape, demonstrating a proportionality between the amplitudes of output and input; this need not necessarily imply that the constant of proportionality must be frequency-independent, however. Secondly, the undistorted passage of a sawtooth waveform, containing not only the fundamental frequency but also its higher harmonics, implies the occurrence of linearization in the "Hi-Fi" sense that the system becomes nondispersive within a certain frequency range when the noise intensity is large enough.

The physical origin of both forms of signal restoration can readily be understood, at least qualitatively, in the following terms. Where the amplitude response of a system to a periodic force is nonlinear, this arises because the amplitude of the vibrations induced by the force is comparable with, or larger than, some characteristic nonlinear length scale of the system, determined by the structure of the region of phase space being visited. The effect of noise is to smear the system over a larger region of phase space, so that a variety of different scales and frequencies then become involved in the motion, even in the absence of periodic driving, and the effective characteristic scale will usually increase as a result. For sufficiently large noise intensities, therefore, the amplitude of the force-induced vibrations will become small compared to the scale (e.g., small compared to the average size of the noise-induced fluctuations), so that the nonlinearity of the

Authorized licensed use limited to: Lancaster University Library. Downloaded on February 28,2010 at 05:33:11 EST from IEEE Xplore. Restrictions apply.

response is correspondingly reduced. Because the system is then spending an increasing proportion of its time far away from its attractor(s), at coordinate values where the timescale that characterizes the motion will in general be quite different and sometimes shorter than for small noise intensities, there will be one or more ranges of frequency for which dispersion is likely to decrease [77]. Although the linearization and the suppression of the dispersion arise, ultimately through the same physical processes, there is no reason to expect that they will become important at the same noise intensity. Dykman *et al.* [73] and Stocks *et al.* [77] have given detailed analyzes of noise-induced linearization phenomena in the standard SR system, with overdamped Brownian motion in the bistable quartic potential (21).

IV. Conclusion

The above examples are intended to convey some idea of the versatility, convenience, and power of analog electronic modeling as a complement to analytic and numerical methods for the investigation of SR and related phenomena. It is equally useful for other phenomena involving noise and nonlinearity where theoretical treatments are necessarily approximate and direct experimental tests are therefore essential. Despite its simplicity, the technique can be applied usefully to problems at the forefront of statistical mechanics as well as to a wide range of applied research.

Acknowledgment

The authors acknowledge, with pleasure, their very considerable indebtedness to M. I. Dykman, I. Kh. Kaufman, S. M. Soskin, and N. D. Stein, who were collaborators in much of the research described in these two papers.

References

[1] D. G. Luchinsky, R. Mannella, P. V. E. McClintock, and N. G. Stocks, "Stochastic resonance in electrical circuits—I: Conventional stochastic resonance," see this issue, pp. 1205–1214.

[2] M. I. Dykman, D. G. Luchinsky, R. Mannella, P. V. E. McClintock, N. D. Stein, and N. G. Stocks, "High-frequency stochastic resonance in periodically-driven systems," *JETP Lett.*, vol. 58, no. 2, pp. 150–156, 1993.

[3] M. I. Dykman, D. G. Luchinsky, R. Mannella, P. V. E. McClintock, N. D. Stein, and N. G. Stocks, "Supernarrow spectral peaks and high-frequency stochastic resonance in systems with coexisting periodic attractors," *Phys. Rev. E*, vol. 49, no. 2, pp. 1198–1215, 1994.

[4] H. Gibbs, *Optical Bistability: Controlling Light with Light*. New York: Academic, 1985.

[5] P. D. Drummond and D. F. Walls, "Quantum theory of optical bistability. I: Nonlinear polarisability model," *J. Phys. A*, vol. 13, pp. 725–741, 1980.

[6] C. Flytzanis and C. L. Tang, "Light-induced critical behavior in the four-wave interaction in nonlinear systems," *Phys. Rev. Lett.*, vol. 45, pp. 441–445, 1980.

[7] J. A. Goldstone and E. Garmire, "Intrinsic optical bistability in nonlinear media," *Phys. Rev. Lett.*, vol. 53, no. 9, pp. 910–913, 1984.

[8] G. Gabrielse, H. Dehmelt, and W. Kells, "Observation of a relativistic, bistable hysteresis in the cyclotron motion of a single electron," *Phys. Rev. Lett.*, vol. 54, no. 6, pp. 537–539, 1985.

[9] H. Dehmelt, "Experiments with an isolated subatomic particle at rest," *Rev. Mod. Phys.*, vol. 62, no. 3, pp. 525–530, 1990.

[10] M. I. Dykman and M. A. Krivoglaz, "Theory of the fluctuational transitions between the stable states of a nonlinear oscillator," *Sov. Phys.—JETP*, vol. 50, pp. 30–37, 1979.

[11] L. D. Landau and E. M. Lifshitz, *Mechanics*. London, U.K.: Pergamon, 1976.

[12] H. Kramers, "Brownian motion in a field of force and the diffusion model of chemical reactions," *Physica (Utrecht)*, vol. 7, pp. 284–304, 1940.

[13] M. I. Dykman, R. Mannella, P. V. E. McClintock, and N. G. Stocks, "Fluctuation-induced transitions between periodic attractors—Observation of supernarrow spectral peaks near a kinetic phase-transition," *Phys. Rev. Lett.*, vol. 65, no. 1, pp. 48–51, 1990.

[14] M. I. Dykman and M. A. Krivoglaz, "Theory of nonlinear oscillator interacting with a medium," in *Soviet Physics Reviews*, M. I. Khalatnikov (Ed.). New York: Harwood Academic, 1984, vol. 5, pp. 265–442.

[15] S. M. Soskin, "Fluctuation spectrum peaks for systems where the oscillation frequency dependence on energy has an extremum," *Physica A*, vol. 155, pp. 401–429, 1989.

[16] S. M. Soskin, "Evolution of zero-dispersion peaks in fluctuation spectra with temperature," *Physica A*, vol. 180, no. 00, pp. 386–406, 1992.

[17] N. G. Stocks, N. D. Stein, S. M. Soskin, and P. V. E. McClintock, "Zero-dispersion stochastic resonance," *J. Phys. A: Math. Gen.*, vol. 25, no. 18, pp. L1119–L1125, 1992.

[18] N. G. Stocks, N. D. Stein, and P. V. E. McClintock, "Stochastic resonance in monostable systems," *J. Phys. A: Math. Gen.*, vol. 26, no. 7, pp. L385–L390, 1993.

[19] R. Barone and G. Paterno, *Physics and Applications of the Josephson Effect*. New York: Wiley, 1982.

[20] I. Kh. Kaufman, D. G. Luchinsky, P. V. E. McClintock, S. M. Soskin, and N. D. Stein, "High-frequency stochastic resonance in SQUID's," *Phys. Lett. A*, vol. 220, nos. 4–5, pp. 219–223, 1996.

[21] P. V. E. McClintock, S. M. Soskin, N. D. Stein, and N. G. Stocks, "Universality of zero-dispersion peaks in the fluctuation spectra of underdamped nonlinear oscillators," *Phys. Rev. E*, vol. 48, no. 1, pp. 147–156, 1993.

[22] G. P. Golubev, I. Kh. Kaufman, D. G. Luchinsky, P. V. E. McClintock, S. M. Soskin, and N. D. Stein, "Zero-dispersion stochastic resonance in underdamped SQUID's," *Int. J. Bifurc. Chaos*, vol. 8, no. 4, pp. 843–848, 1998.

[23] I. Kh. Kaufman, D. G. Luchinsky, P. V. E. McClintock, S. M. Soskin, and N. D. Stein, "Zero-dispersion stochastic resonance in a model for a superconducting quantum interference device," *Phys. Rev. E*, vol. 57, no. 1, pp. 78–87, 1998.

[24] A. D. Hibbs, A. L. Singsaas, E. W. Jacobs, A. R. Bulsara, J. J. Bekkedahl, and F. Moss, "Stochastic resonance in a superconducting loop with a Josephson-junction," *J. Appl. Phys.*, vol. 77, no. 6, pp. 2582–2590, 1995.

[25] M. I. Dykman, D. G. Luchinsky, P. V. E. McClintock, N. D. Stein, and N. G. Stocks, "Stochastic resonance for periodically-modulated noise intensity," *Phys. Rev. A*, vol. 46, no. 4, pp. R1713–R1716, 1992.

[26] S. Fauve and F. Heslot, "Stochastic resonance in a bistable system," *Phys. Lett. A*, vol. 97, nos. 1–2, pp. 5–7, 1983.

[27] R. Benzi, A. Sutera, and A. Vulpiani, "The mechanism of stochastic resonance," *J. Phys. A*, vol. 14, no. 11, pp. L453–L457, 1981.

[28] Z. Gingl, L. B. Kiss, and F. Moss, "Non-dynamical stochastic resonance:theory and experiments with white and arbitrarily colored noise," *Europhys. Lett.*, vol. 29, pp. 191–196, 1995.

[29] Z. Gingl, L. B. Kiss, and F. Moss, "Non-dynamical stochastic resonance:theory and experiments with white and various colored noises," *Nuovo Cimento D*, vol. 17, pp. 795–802, 1995.

[30] K. Wiesenfeld and K. DeMino, "Single-trigger stochastic resonance," *Nuovo Cimento D*, vol. 17, nos. 7–8, pp. 977–981, 1995.

[31] L. Gammaitoni, "Stochastic resonance and the dithering effect in threshold physical systems," *Phys. Rev. E*, vol. 52, no. 5, pp. 4691–4698, 1995.

[32] X. Godivier and F. Chapeau-Blondeau, "Intrinsic optical bistability in nonlinear media," *Signal Processing*, vol. 56, no. 3, pp. 293–303, 1997.

[33] J. J. Collins, C. C. Chow, and T. T. Imhoff, "Stochastic resonance without tuning," *Nature*, vol. 376, no. 6537, pp. 236–238, 1995.

[34] G. Hu, D. C. Gong, X. D. Wen, C. Y. Yang, G. R. Qing, and R. Li, "Stochastic resonance in a nonlinear systems driven by an aperiodic force," *Phys. Rev. A.*, vol. 46, no. 6, pp. 3250–3254, 1992.

[35] M. DeWeese and W. Bialek, "Information-flow in sensory neurons," *Nuovo Cimento D*, vol. 17, nos. 7–8, pp. 733–741, 1995.

[36] A. R. Bulsara and A. Zador, "Threshold detection of wideband signals: A noise-induced maximum in the mutual information," *Phys. Rev. E.*, vol. 54, no. 3, pp. R2185–R2188, 1996.

[37] C. Heneghan, C. C. Chow, J. J. Collins, T. T. Imhoff, S. B. Lowen, and M. C. Teich, "Information measures quantifying aperiodic stochastic resonance," *Phys. Rev. E.*, vol. 54, no. 3, pp. R2228–R2231, 1996.

[38] F. Chapeau-Blondeau, "Noise-enhanced capacity via stochastic resonance in an asymmetric binary channel," *Phys, Rev. E*, vol. 55, no. 2, pp. 2016–2019, 1997.

Authorized licensed use limited to: Lancaster University Library. Downloaded on February 28,2010 at 05:33:11 EST from IEEE Xplore. Restrictions apply.

[39] X. Godivier and F. Chapeau-Blondeau, "Stochastic resonance in the information capacity of a nonlinear dynamical system," *Int. J. Bifur. Chaos*, vol. 8, no. 3, pp. 581–589, 1998.

[40] G. Deco and B. Schurmann, "Stochastic resonance in the mutual information between input and output spike trains of a central neuron," *Physica D*, vol. 17, nos. 1–4, pp. 276–282, 1998.

[41] L. Schimansky-Geier, J. A. Freud, A. B. Neiman, and B. Shulgin, "Noise induced order: Stochastic resonanc," *Int. J. Bifurc. Chaos*, vol. 8, no. 5, pp. 869–879, 1998.

[42] A. R. Bulsara and G. Schmera, "Stochastic resonance in globally coupled nonlinear oscillators," *Phys. Rev. E*, vol. 47, no. 5, pp. 3734–3737, 1993.

[43] M. E. Inchiosa and A. R. Bulsara, "Nonlinear dynamic elements with noisy sinusoidal forcing—Enhancing response via nonlinear coupling," *Phys. Rev. E*, vol. 52, no. 1, pp. 327–339, 1995.

[44] M. E. Inchiosa and A. R. Bulsara, "Signal detection statistics of stochastic resonators," *Phys. Rev. E*, vol. 53, no. 3, pp. R2021–R2024, 1996.

[45] W. J. Rappel and A. Karma, "Noise-induced coherence in neural networks," *Phys. Rev. Lett.*, vol. 77, no. 15, pp. 3256–3259, 1996.

[46] J. Pham, K. Pakdaman, and J. F. Vibert, "Noise-induced coherence in randomly connected neural networks," *Phys. Rev. E*, vol. 58, no. 3, pp. 3610–3622, 1998.

[47] J. F. Lindner, B. K. Meadows, W. L. Ditto, M. E. Inchiosa, and A. R. Bulsara, "Array enhanced stochastic resonance and spatiotemporal synchronization," *Phys. Rev. Lett.*, vol. 75, no. 1, pp. 3–6, 1995.

[48] M. Locher, G. A. Johnson, and E. R. Hunt, "Spatiotemporal stochastic resonance in a system of coupled diode resonators," *Phys. Rev. Lett.*, vol. 77, no. 23, pp. 4698–4701, 1996.

[49] F. Mar.esoni, L. Gammaitoni, and A. R. Bulsara, "Spatiotemporal stochastic resonance in a phi(4) model of kink antikink nucleation," *Phys. Rev. Lett.*, vol. 76, no. 15, pp. 2609–2612, 1996.

[50] M. Locher, D. Cigna, E. R. Hunt, F. Johnson, G. A. Maresoni, L. Gammaitoni, M. E. Inchiosa, and A. R. Bulsara, "Stochastic resonance in coupled nonlinear dynamic elements," *Chaos*, vol. 8, no. 3, pp. 604–615, 1998.

[51] M. Locher, D. Cigna, and E. R. Hunt, "Noise sustained propagation of a signal in coupled bistable elements," *Phys. Rev. Lett.*, vol. 80, no. 23, pp. 5212–5215, 1998.

[52] U. Siewert and L. Schimansky-Geier, "Analytical study of coupled two-state stochastic resonators," *Phys. Rev. E*, vol. 58, no. 3, pp. 2843–2852, 1998.

[53] J. F. Lindner, S. Chandramouli, A. R. Bulsara, M. Locher, and W. L. Ditto, "Noise enhanced propagation," *Phys. Rev. Lett.*, vol. 81, no. 23, pp. 5048–5051, 1998.

[54] E. Pantazelou, F. Moss, and D. Chialvo, *Noise in Physical Systems and* $1/f$ *Noise*. New York: American Institute of Physics, 1993, pp. 549–552.

[55] X. Pei, L. Wilkens, and F. Moss, "Noise-mediated spike timing precision from aperiodic stimuli in an array of Hodgekin-Huxley-type neurons," *Phys. Rev. Lett.*, vol. 77, no. 22, pp. 4679–4682, 1996.

[56] D. R. Chialvo, A. Longtin, and J. Muller-Gerking, "Stochastic resonance in models of neuronal ensembles," *Phys. Rev. E*, vol. 55, no. 2, pp. 1798–1808, 1997.

[57] P. C. Gailey, A. Neiman, J. J. Collins, and F. Moss, "Stochastic resonance in the ensembles of nondynamical elements: The role of internal noise," *Phys. Rev. Lett.*, vol. 79, no. 23, pp. 4701–4704, 1997.

[58] R. Fakir, "Nonstationary stochastic resonance," *Phys. Rev. E*, vol. 57, no. 6, pp. 6996–7001, 1998.

[59] S. K. Han, W S. Kim, and H. Kook, "Temporal segmentation of the stochastic oscillator neural network," *Phys. Rev. E*, vol. 58, no. 2, pp. 2325–2334, 1998.

[60] M. Riani and E. Simonotto, "Stochastic resonance in the perceptual interpretation of ambigous figures—A neural network model," *Phys. Rev. Lett.*, vol. 72, no. 19, pp. 3120–3123, 1994.

[61] M. Spitzer and M. Neumann, "Noise in models of neurological and psychiatric disorders," *Int. J. Neural Syst.*, vol. 7, no. 4, pp. 355–361, 1996.

[62] A. N. Grigorenko, P. I. Nikitin, and G. V. Roshchepkin, "A new technique for high-frequency sub-threshold magnetic field sensing in nanometer scale based upon magnetostochastic resonance," *Sens. Actuators A-Phys.*, vol. 59, nos. 1–3, pp. 277–279, 1997.

[63] J. K. Douglass, L. Wilkens, E. Pantazelou, and F. Moss, "Noise-enhancement of information-transfer in crayfish mechanoreceptors by stochastic resonance," *Nature*, vol. 365, no. 6444, pp. 337–441, 1993.

[64] F. Y. Chiou Tan, K. N. Magee, L. R. Robinson, M. R. Nelson, and S. S. Tuel, "Augmented sensory nerve action potentials during muscle tension mediated noise," *Int. J. Bifurc. Chaos*, vol. 6, no. 7, pp. 1389–1396, 1996.

[65] N. G. Stocks, "Suprathreshold stochastic resonance in multi-level threshold systems," *PRL*, submitted for publication.

[66] V. R. Algazi, "Useful approximations to optimal quantization," *IEEE Trans. Commun. Theory*, vol. COM-14, pp. 297–301, 1966.

[67] J. A. Bucklew, "Companding and random quantization in several dimensions," *IEEE Trans. Inform. Theory*, vol. 27, pp. 207–211, 1998.

[68] M. Abramowitz and I. A. Stegun, *Handbook of Mathematical Functions*. New York: Dover, 1972, p. 297.

[69] N. G. Stocks, "A new method for noise-enhanced information encoding in ADCs," unpublished.

[70] M. I. Dykman, G. P. Golubev, D. G. Luchinsky, P. V. E. McClintock, N. D. Stein, and N. G. Stocks, "Noise-enhanced heterodyning in bistable systems," *Phys. Rev. E*, vol. 49, no. 3, pp. 1935–1942, 1994.

[71] M. I. Dykman, G. P. Golubev, I. Kh. Kaufman, D. G. Luchinsky, P. V. E. McClintock, and E. A. Zhukov, "Noise-enhanced optical heterodyning in an all-optical bistable system," *Appl. Phys. Lett.*, vol. 67, no. 3, pp. 308–310, 1995.

[72] M. I. Dykman, G. P. Golubev, I. Kh. Kaufman, D. G. Luchinsky, P. V. E. McClintock, and E. A. Zhukov, "Fluctuations, stochastic resonance and noise-protected heterodyning in bistable optical-systems," *Nuovo Cimento D*, vol. 17, nos. 7–8, pp. 743–754, 1995.

[73] M. I. Dykman, D. G. Luchinsky, R. Mannella, P. V. E. McClintock, H. E. Short, N. D. Stein, and N. G. Stocks, "Noise-induced linearization," *Phys. Lett. A*, vol. 97, pp. 61–66, 1994.

[74] A. S. French, A. V. Holden, and R. B. Stein, "The estimation of the frequency response function of a mechanoreceptor," *Kybernetik*, vol. 11, pp. 15–23, 1972.

[75] K. Vogel, H. Risken, W. Schleich, M. James, F. Moss, R. Mannella, and P. V. E. McClintock, "Colored noise in the ring-laser gyroscope—Theory and simulation," *J. Appl. Phys.*, vol. 62, no. 2, pp. 721–723, 1987.

[76] M. Millonas (Ed.), *Fluctuations and Order: The New Synthesis*. Berlin, Germany: Springer-Verlag, 1996.

[77] N. G. Stocks, N. D. Stein, H. E. Short, P. V. E. McClintock, R. Mannella, D. G. Luchinsky, and M. I. Dykman, "Noise-induced linearization and delinearization," in *Fluctuations and Order: The New Synthesis*, M. Millonas (Ed.). Berlin, Germany: Springer-Verlag, 1996, pp. 53–68.

Dmitrii G. Luchinsky, for a photograph and biography, see this issue, p. 1214.

Riccardo Mannella, for a photograph and biography, see this issue, p. 1214.

Peter V. E. McClintock, for a photograph and biography, see this issue, p. 1214.

Nigel G. Stocks, for a photograph and biography, see this issue, p. 1214.

Authorized licensed use limited to: Lancaster University Library. Downloaded on February 28,2010 at 05:33:11 EST from IEEE Xplore. Restrictions apply.